

# Calibration of the Watermark 200SS moisture sensor for irrigation scheduling in five soil types in Zacatecas, Mexico

Servin-Palestina, Miguel<sup>1\*</sup>; Vargas-Cano, David<sup>2\*</sup>; García-Martínez, Jesús A.<sup>2</sup>; Ramírez-Valle, Orlando<sup>3</sup>; Jiménez-Jiménez, Sergio I.<sup>4</sup>; Reyes-Gonzales, Arturo<sup>5</sup>

<sup>1</sup> Instituto Nacional de Investigaciones Forestales, Agrícolas y Pecuarias (INIFAP-CEZAC). Calera de V. R., Zacatecas, México. C. P. 98500.

<sup>2</sup> Universidad Autónoma de Zacatecas. Zacatecas, México. C. P. 98000

<sup>3</sup> Instituto Nacional de Investigaciones Forestales Agrícolas y Pecuarias (INIFAP-CESICH). Cd. Cuauhtémoc, Chihuahua, México. C. P. 31500

<sup>4</sup> Instituto Nacional de Investigaciones Forestales Agrícolas y Pecuarias (INIFAP-CENID-RASPA), Gómez Palacio 35079, Durango, México

<sup>5</sup> Instituto Nacional de Investigaciones Forestales, Agrícolas y Pecuarias (INIFAP-CELALA), Matamoros, Coahuila, México. C.P. 27440

\* Correspondence: servin.miguel@inifap.gob.mx, d.v.c.cano@gmail.com

## ABSTRACT

**Objective:** To develop an irrigation scheduling methodology based on the calibration of WATERMARK 200SS sensors, aimed at optimizing water use for six key crops garlic, chili, maize, oats, alfalfa, and beans in agricultural soils of Zacatecas, Mexico, considering their hydro-physical properties and specific crop water requirements.

**Design/methodology/approach:** Five soil types were characterized based on bulk density, texture, organic matter content, and water retention curves using the van Genuchten model. WATERMARK sensors were calibrated through polynomial models ( $R^2 > 0.96$ ) to correlate sensor readings (centibars, cbar) with gravimetric soil moisture content. The proposed irrigation scheduling framework integrated: (1) soil water balance, (2) critical tension thresholds (0.3-1.0 atm), and (3) real-time sensor data, tailored for drip irrigation systems operating at 95% efficiency.

**Results:** Clay soils (Samples 1 and 5) demonstrated greater water retention capacity ( $H_s$  up to  $0.231 \text{ cm}^3/\text{cm}^3$ ), whereas sandy loam soil (Sample 2) exhibited rapid drainage ( $\alpha = 0.022$ ). Calibration curves for the sensors achieved high precision ( $\text{RMSE} < 0.007$ ), ensuring accurate estimation of soil moisture within optimal agronomic thresholds, spanning from field capacity to the permanent wilting point. Irrigation depths were determined per crop, based on soil water tension data derived from the calibrated sensors.

**Limitations/implications:** The methodology necessitates *in situ* calibration for each soil type and does not address uncontrolled spatial variability. Nevertheless, it offers a practical and scalable solution for farmers in arid regions, reducing dependence on empirical irrigation methods.

**Findings/conclusions:** WATERMARK 200SS sensors, when calibrated using localized models, effectively enable precision irrigation scheduling. This methodology significantly improves water-use efficiency across essential crops, providing resilience against climatic stressors in the semi-arid context of Zacatecas.

**Keywords:** Irrigation scheduling, soil moisture sensors, WATERMARK 200SS, soil water retention curve, sensor calibration.

**Citation:** Servin-Palestina, M., Vargas-Cano, D., García-Martínez, J. A., Ramírez-Valle, O., Jiménez-Jiménez, S. I., & Reyes-Gonzales, A. (2025). Calibration of the Watermark 200SS moisture sensor for irrigation scheduling in five soil types in Zacatecas, Mexico. *Agro Productividad*. <https://doi.org/10.32854/tpnv7y27>

**Academic Editor:** Jorge Cadena Iñiguez

**Associate Editor:** Dra. Lucero del Mar Ruiz Posadas

**Guest Editor:** Daniel Alejandro Cadena Zamudio

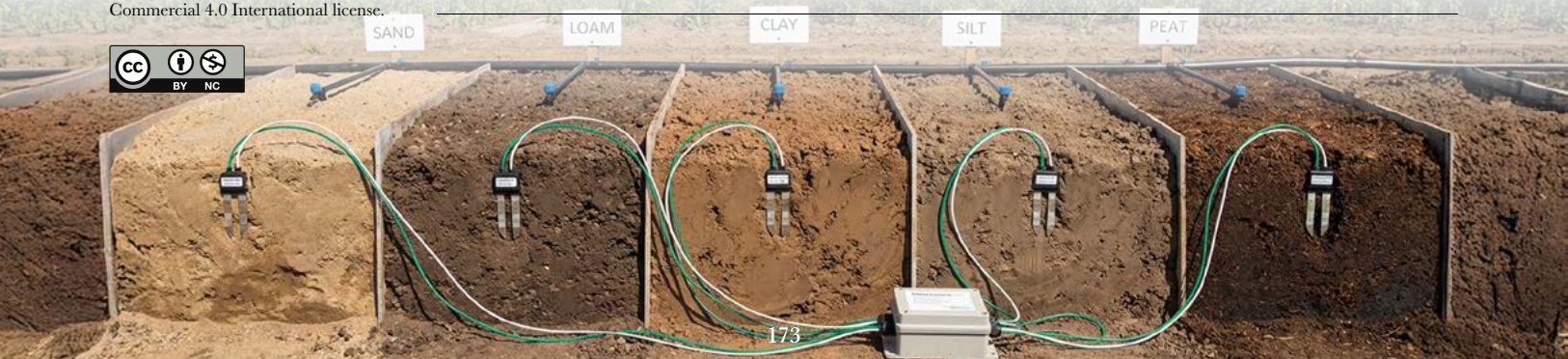
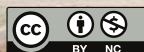
**Received:** June 28, 2025.

**Accepted:** October 24, 2025.

**Published on-line:** December XX, 2025.

*Agro Productividad*, 18(11). November. 2025. pp: 173-185.

This work is licensed under a Creative Commons Attribution-Non-Commercial 4.0 International license.



## INTRODUCTION

Water is one of the most limited and essential natural resources for human development, playing a vital role in agricultural production, economic growth, and social well-being. As the global population increases, so does the demand for water both for food production and for meeting domestic consumption needs (Kılıç, 2020). This pressure is further exacerbated by climate variability, which has intensified the frequency and severity of events such as droughts and extreme temperatures, particularly in the arid and semi-arid regions of Zacatecas (Guzmán-López *et al.*, 2024). In this context, the implementation of efficient irrigation techniques is essential to optimize water use while alleviating stress on aquifers and ensuring the sustainability of this critical resource (Torres-Moreno *et al.*, 2023). Irrigation scheduling, which determines when and how much to irrigate, has traditionally been based on growers' intuition and empirical experience, often without technical support and relying solely on practical knowledge (Servín *et al.*, 2017; Bórquez-López *et al.*, 2013). However, recent advances have introduced more technical approaches, including climatic water balance, crop water stress indices, and soil moisture sensors. These methods require a precise understanding of crop water needs and soil-water dynamics. Although they offer greater accuracy in water management, their implementation must be tailored to the specific conditions of each region and cropping system, necessitating sensor calibration according to local soil and water characteristics (Abdelfattah *et al.*, 2020). Soil moisture retention capacity determines how much water is available to plants and depends on physical soil properties and phenomena such as adhesion and surface tension. This retention is measured as matric potential, expressed in pressure units, and defines key points: field capacity, which represents the maximum water held against gravity, and the permanent wilting point, at which plants can no longer absorb water (Chavarría-Vidal *et al.*, 2024). Understanding this retention force is essential for establishing soil water retention curves, which describe the relationship between soil water content and the energy with which it is retained. Maintaining soil moisture within an optimal range is crucial to prevent issues such as pest outbreaks, root rot, nutrient leaching (Bedard-Haughn, 2009; Tudor *et al.*, 2013), and, conversely, water stress. Water tension thresholds vary by crop; for example, in garlic, chili, maize, oats, alfalfa, and beans, they typically range from 0.3 to 1.0 atmospheres (atm), depending on soil conditions, climate, and crop growth stage. Soil moisture sensors are effective tools for irrigation monitoring and scheduling. However, to ensure reliable readings, they require thorough calibration that accounts for specific edaphic conditions, as sensor response varies significantly with soil texture and composition (Galdeano *et al.*, 2024). The Watermark 200SS<sup>®</sup> sensor, in particular, is widely used due to its versatility, ease of installation, and accuracy in measuring soil water matric potential (Medina *et al.*, 2018). Therefore, the aim of this study was to calibrate the Watermark sensor by correlating its readings with volumetric water content in five distinct soil types from Zacatecas, Mexico. This calibration allowed the establishment of crop- and soil-specific sensor thresholds to determine precise irrigation timing and depth, enabling water-efficient irrigation scheduling adapted to crop water requirements.

## MATERIALS AND METHODS

### Study area description

This study was conducted at the Zacatecas Experimental Field (CE-ZAC-INIFAP). Soil samples were collected from five agricultural sites across the state of Zacatecas during the last week of January 2024. Approximately 100 kg of soil were obtained per site, sampled at a depth ranging from 10 to 40 cm.

### Physical characterization and soil water properties

#### Bulk density

The *in-situ* bulk density of the five soils was determined using the core method. The procedure was performed in triplicate at each site using cylindrical cores with a diameter of 5.12 cm and a height of 6.1 cm, corresponding to a volume of 125.8 cm<sup>3</sup>. Care was taken to avoid additional compaction during sampling to ensure the accuracy of the results. Soil samples were placed in labeled plastic bags and subsequently oven-dried at 105 °C for 24 hours until reaching a constant weight. The dry mass was then used to calculate the soil bulk density (Equation 1).

$$D = \frac{M}{V} \quad (1)$$

Where:  $D$  is the bulk density (g cm<sup>-3</sup>);  $M$  is the dry soil mass (g), and  $V$  is the volume of the cylinder (cm<sup>3</sup>).

#### Soil texture and organic matter content

Soil classification was performed using the soil texture triangle and the percentages of sand, silt, and clay determined through laboratory analysis using the Bouyoucos hydrometer method (AS-09). Organic matter content was assessed via the Walkley and Black method (AS-07), which involves the oxidation of organic carbon using potassium dichromate and concentrated sulfuric acid. Both methods comply with the Mexican Official Standard PROY-NOM-021-RECNAT-2000.

#### Construction of the soil water retention curve

Soil water retention capacity under varying tensions was determined using the pressure plate method (Richards' apparatus) on 1 kg samples from each soil type. This procedure,

**Table 1.** Location of agricultural sampling sites in the state of Zacatecas, Mexico.

Sample	Latitude	Longitude	Agricultural Zone (Zacatecas)
Sample 1	23.04295766	-102.336794	Chaparrosa
Sample 2	23.372474	-102.883494	Plateros
Sample 3	23.362264	-102.991591	Altamira
Sample 4	23.14617354	-102.719598	Pardillo Tercero
Sample 5	23.08122635	-102.314767	Chaparrosa

described in the Mexican Official Standard PROY-NOM-021-RECNAT-2000 (AS-06), allowed for the construction of water retention curves by applying suction levels of 0.3, 1.0, 3.0, 5.0, 9.0, and 15.0 atmospheres. The corresponding moisture content at each tension level was determined using the gravimetric method (Equation 2).

$$H = \frac{PSH - PSS}{PSS} \times 100 \quad (2)$$

Where:  $H$  is the gravimetric moisture content (%);  $PSH$  is the wet soil weight (g), and  $PSS$  is the dry soil weight (g).

The results were plotted to generate soil water retention curves, which were fitted using the van Genuchten model, applying the constraint  $m = 1 - 1/n$  (Equation 3).

$$\widehat{H} = h_r + \frac{h_s - h_r}{(1 + aT^n)^m} \quad (3)$$

Where:  $\widehat{H}$  is the predicted moisture content (g/g);  $h_r$  is the residual moisture (g/g);  $h_s$  is the saturation moisture content (g/g);  $a$  is an empirical parameter;  $T$  is the applied tension (atm), and  $m$  and  $n$  are fitting parameters.

### Calibration of WATERMARK Sensors

The WATERMARK sensor is a granular matrix sensor that operates based on electrical resistance. It consists of a porous block containing two embedded metal electrodes (Tartaglia *et al.*, 2023). Measurements were obtained using the WATERMARK<sup>®</sup> digital meter (Model 30-KTCD-NL, Irrrometer Company Inc., Riverside, CA), a portable device specifically designed for field reading of WATERMARK<sup>®</sup> sensors.

The meter provides digital readings in centibars (cbar), reflecting soil water tension, which corresponds to the energy a plant's root system must exert to extract water from the soil. Higher tension values indicate drier soil conditions, while lower values correspond to wetter soils (Irrrometer, 2024).

### Calibration

The calibration of WATERMARK<sup>®</sup> soil moisture sensors (200SS, Irrrometer Company Inc., Riverside, CA) was carried out following the protocol for porous media sensor calibration developed by Soham *et al.* (2019). The calibration procedure (Figure 1) involved placing dry soil samples into PVC containers (6" diameter × 30 cm height) equipped with a mesh at the base to allow drainage. The dry soil weight (PSS) was recorded prior to saturation, and a WATERMARK 200SS sensor was inserted into each container.

The soil was saturated via capillarity until a reading of 0 cbar was reached, after which it was allowed to drain freely. Periodic measurements of wet soil weight (PSH) were taken using a digital scale (LEQ-10-N, Torrey, Mexico) to calculate the gravimetric moisture content (Equation 2). Disturbed soil samples were used (*i.e.*, pre-sieved before calibration),

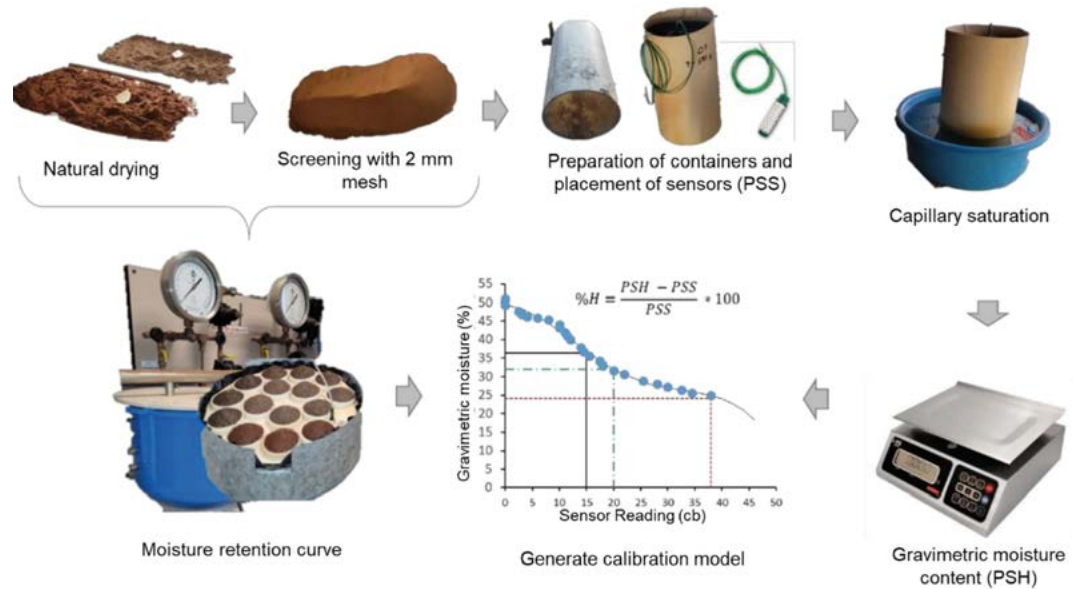


**Figure 1.** Conceptual diagram of the soil moisture sensor calibration process.

as recommended by Starr and Paltineanu (2002), who noted that using disturbed soils enhances calibration accuracy for moisture sensors.

A fourth-order polynomial model (Equation 5) was then fitted to describe the relationship between soil moisture content and the corresponding sensor reading.

$$y = -ax^4 + bx^3 - cx^3 - dx + e \tag{5}$$

Where:  $y$  is the measured soil moisture content in percentage (g/g);  $x$  is the WATERMARK sensor reading (cbar); and  $a, b, c, d,$  and  $e$  are the coefficients of the polynomial model.

**Irrigation Scheduling**

Irrigation scheduling was developed using an integrated approach based on: (1) soil water balance, (2) crop water requirements, and (3) real-time data from soil moisture sensors. The primary objective was to maintain soil moisture content within the optimal range between field capacity and the permanent wilting point to ensure water availability for crops while avoiding both water deficits and excesses that could impair plant development (Catalán *et al.*, 2007). Additionally, irrigation was guided by the optimal soil water tension for each crop.

This methodology was applied to six representative crops in the study area: garlic (*Allium sativum*), chili pepper (*Capsicum annum*), maize (*Zea mays*), oats (*Avena sativa*), alfalfa (*Medicago sativa*), and common bean (*Phaseolus vulgaris*). Initial irrigation depth ( $L_{ini}$ ) for crop establishment was calculated using Equation 4, assuming a drip irrigation system operating at 95% efficiency.

$$L_{ini} = (H_{CC} - H_{PMP}) \cdot Da \cdot Z \tag{4}$$

Where:  $H_{CC}$  is the soil moisture at field capacity (g/g);  $H_{PMP}$  is the soil moisture at the permanent wilting point (g/g);  $Da$  is the soil bulk density, and  $Z$  is the effective rooting depth (e.g., 40 cm for garlic).

In addition, sensor readings in centibars were used to maintain soil moisture within the crop-specific optimal range. The maximum depletion fraction (FAM) *i.e.*, the amount of water that can be extracted from the soil before triggering the next irrigation event was also calculated (Servín *et al.*, 2017).

## RESULTS AND DISCUSSION

### Bulk density

Bulk density is a key indicator of soil health, as it reflects the degree of compaction and porosity. High bulk density ( $Da$ ) values are typically associated with compaction problems, which can limit water infiltration, reduce aeration, and hinder root development (Hargreaves *et al.*, 2019). Conversely, low bulk density may indicate high porosity, but it can also suggest a risk of erosion or elevated organic matter content. The results (Table 2) revealed significant differences among the sampling sites. Sample 2 exhibited the highest bulk density ( $1.56 \text{ g cm}^3 \pm 0.089$ ), suggesting potential restrictions to root growth, in accordance with USDA (1999) guidelines. In contrast, Sample 5 showed the lowest bulk density ( $1.00 \text{ g cm}^3 \pm 0.048$ ), indicating a more porous structure with reduced compaction. This may be attributed to higher organic matter content and the application of soil conservation practices.

### Texture and organic matter

The analyzed soils exhibited significant textural variability, which directly influenced their organic matter (OM) content (Table 3). Clay soils (Samples 1 and 5) showed intermediate OM values (2.04-2.13%), consistent with their higher capacity to retain nutrients and stabilize carbon. In contrast, the sandy loam soil (Sample 2) recorded the lowest OM content (0.67%), attributable to its high sand fraction (65.8%). Notably, Sample 4, which has a balanced texture of sand, clay, and silt, presented the highest OM content (3.29%). This suggests that additional factors, such as agricultural management or biomass inputs, may be enhancing carbon accumulation. These findings support the

**Table 2.** Parent Density obtained by the cylinder method in five soils sampled in agricultural areas of the state of Zacatecas, Mexico.

Soil	$Da \text{ (g cm}^{-3}\text{)}$
Sample 1	$1.12 \pm 0.012$
Sample 2	$1.56 \pm 0.089$
Sample 3	$1.24 \pm 0.062$
Sample 4	$1.23 \pm 0.012$
Sample 5	$1.00 \pm 0.048$

**Table 3.** Soil texture and organic matter.

Soil Sample	Sand (%)	Clay (%)	Silt (%)	Texture	Organic Matter (OM, %)
Sample 1	29.8	42.2	28.0	Clay	2.04
Sample 2	65.8	12.2	22.0	Sandy Loam	0.67
Sample 3	37.8	30.2	32.0	Clay Loam	2.33
Sample 4	45.8	30.2	24.0	Sandy Clay Loam	3.29
Sample 5	19.8	54.2	26.0	Clay	2.13

Soil water retention curve.

well-documented relationship between fine-textured soils and higher OM content (Hartati & Sudarmadji, 2016), while exceptions like Sample 4 underscore the need to account for external variables.

The soil water retention curve, which relates soil water content to matric potential, exhibited a characteristic sigmoidal behavior across all five analyzed soils. The van Genuchten model provided an excellent fit to the data ( $R^2 > 98.5\%$ ;  $RMSE < 0.007$ ), confirming its effectiveness in describing water dynamics in these soils (Table 4). Model parameters revealed key differences in water storage and release capacities, associated with the texture and structure of each soil. The van Genuchten parameters highlighted distinct patterns in water retention behavior. High  $\alpha$  values, such as that of Sample 3 (0.078), indicate greater water retention at low tensions a trait of clay loam soils which suggests high plant-available water content. In contrast, the low  $\alpha$  value of Sample 2 (0.022) reflects limited initial retention, consistent with its sandy loam texture (65.8% sand) and rapid drainage capacity. Moreover, high  $n$  values indicate sharper water release as tension increases, typical of soils with more uniform pore size distribution. Elevated  $\theta_s$  (Sample 5: 0.231) and  $\theta_r$  (3.841) values in clay soils demonstrate high total porosity but lower retention under water stress. Conversely, Sample 2, with  $\theta_s = 0.022$  and  $\theta_r = 1.518$ , confirms its poor water retention capability due to its high sand content (Figure 2).

Samples (2 and 4) require more frequent but shorter irrigation cycles to compensate for their low plant-available water and to avoid losses due to percolation. In contrast, clay soils (Samples 1 and 5), while retaining more water overall, exhibit high retention at the permanent wilting point (PWP), which reduces the effective availability of water for plants. For these soils, techniques such as mulching are recommended to improve water-

**Cuadro 4.** Parámetros de modelo van Genuchten de las curvas de retención de humedad de cinco suelos diferentes de Zacatecas, México.

Parameter	Sample 1	Sample 2	Sample 3	Sample 4	Sample 5
$\theta_s$	0.183	0.022	0.026	0.066	0.231
$\theta_r$	3.496	1.518	2.596	2.581	3.841
$\alpha$	0.035	0.022	0.078	0.046	0.041
$n$	0.446	0.602	0.695	0.613	0.533
RMSE	0.003	0.002	0.007	0.005	0.006
$R^2$	0.998	0.985	0.985	0.990	0.993

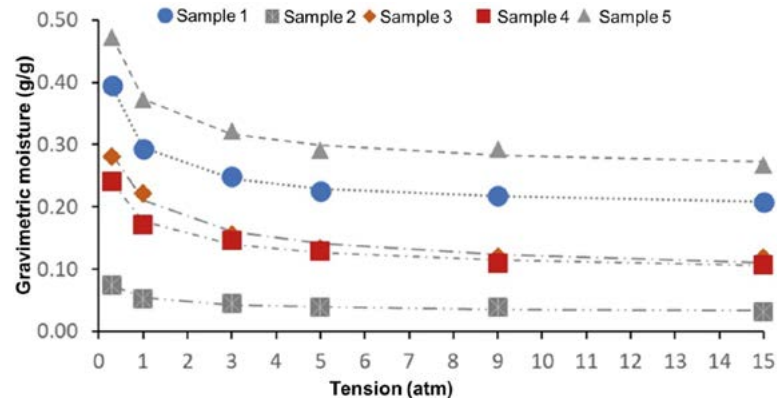


**Figure 2.** Soil water retention curve for five agricultural soils from Zacatecas, Mexico.

use efficiency. Intermediate soils (Sample 3), with a balanced capacity for water storage ( $\alpha=0.078$ ) and gradual release ( $n=0.695$ ), are well-suited for crops with moderate water requirements, offering an optimal balance between retention and aeration.

**Calibration curve of watermark sensors**

The proposed regression models showed excellent fit in relating gravimetric soil moisture (%H) to readings from the WATERMARK sensor, with coefficients of determination ( $R^2$ ) exceeding 0.96 across all five evaluated soils (Table 5). These results confirm the reliability of the sensor in estimating soil water content across a range of textures, from sandy loam (Sample 2) to clay (Sample 5).

The gravimetric soil moisture content (%H) in relation to the WATERMARK<sup>®</sup> sensor reading (Ls) followed a sigmoidal curve, exhibiting a characteristic three-phase pattern (Figure 3):

- Initial Phase: The curve begins with a slow and gradual increase, attributed to the loss of free water under gravitational forces.
- Exponential Growth Phase: A rapid, accelerated increase occurs, corresponding to the range of water that is readily available to plants.
- Final Phase: The curve approaches a maximum value and growth slows again, reflecting the stage where water is more tightly held in the soil matrix, and plants begin to experience water stress.

**Table 5.** Regression model to estimate soil moisture based on sensor readings at five agricultural sites in Zacatecas, Mexico.

ID	Model	R <sup>2</sup>
Sample 1	$y = -0.00004371x^4 + 0.003934x^3 - 0.1025x^2 - 0.02931x + 42.26$	0.99
Sample 2	$y = 0.0000002949x^4 - 0.000111x^3 + 0.01391x^2 - 0.7764x + 19.61$	0.99
Sample 3	$y = -0.00004427x^4 + 0.003788x^3 - 0.09457x^2 - 0.0392x + 36.93$	0.98
Sample 4	$y = -0.00001654x^4 + 0.001265x^3 - 0.01298x^2 - 0.8288x + 28.68$	0.96
Sample 5	$y = -0.000007646x^4 + 0.001588x^3 - 0.06076x^2 - 0.1797x + 53.02$	0.98

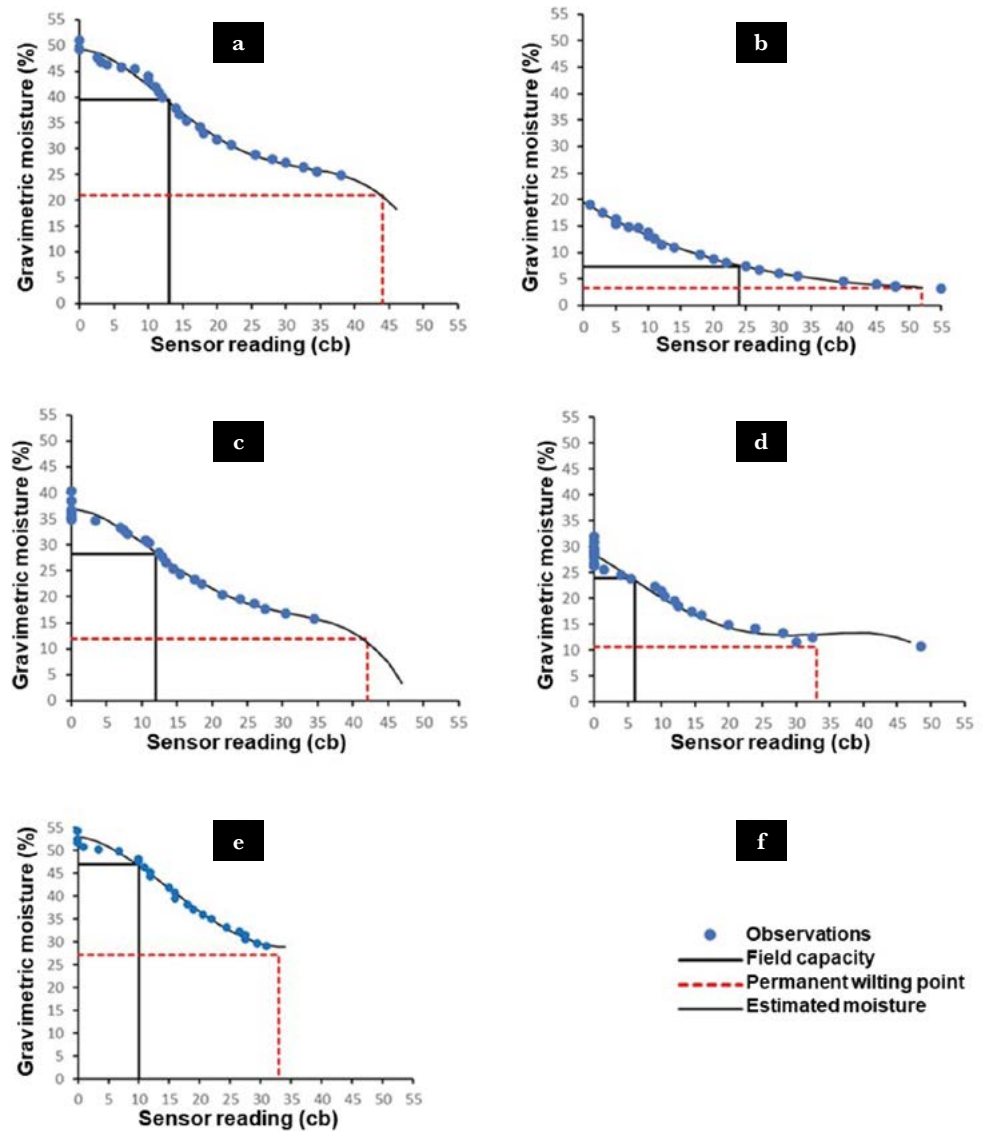


**Figure 3.** Calibration curves of the WATERMARK 200SS moisture sensors for the soils of a) Sample 1, b) Sample 2, c) Sample 3, d) Sample 4, e) Sample 5, and f) interpretation legend.

Additionally, the figure highlights the soil moisture content at field capacity and at the permanent wilting point. The difference between these two thresholds represents the plant-available water.

### Irrigation scheduling with WATERMARK 200SS Sensors

The results (Tables 6, 7, 8, 9, and 10) show the most important parameters to consider for optimal irrigation management, taking into account soil characteristics, crop requirements, and readings from the WATERMARK 200SS sensors. The variability in the evaluated parameters (moisture tension, volumetric moisture, irrigation depths, etc.) reflects the system’s adaptability to different soil conditions and crop water needs. A clear influence of soil properties ( $\theta_{FC}$ ,  $\theta_{PWP}$ ,  $D_b$ ) on irrigation parameters is observed.

In Sample 2 ( $\theta_{FC}=0.12$ ,  $Db=1.56 \text{ g cm}^{-3}$ ), the irrigation depths are significantly lower (7.6-13.01 mm) compared to Sample 1 ( $\theta_{FC}=0.44$ ,  $Db=1.12 \text{ g cm}^{-3}$ ), where LR ranges between 28.88 and 47.06 mm. This is due to the lower water retention capacity in denser soils with lower porosity. In general, soils with high field capacity ( $\theta_{FC}>0.35$ , Samples 1, 3, 5) require less frequent irrigation but with higher depths ( $LR>25 \text{ mm}$ ), while soils with low retention ( $\theta_{FC}<0.30$ , Sample 2) need more frequent irrigation but with lower volume, optimizing water use. Crops with higher water demands, such as maize and alfalfa

**Table 6.** Irrigation programming parameters with WATERMARK 200SS sensors for six crops from sample 1, with  $\theta_{CC}=0.44$ ,  $\theta_{PMP}=0.23$  and  $Da=1.12 \text{ g cm}^{-3}$ .

Crop	Pr (mm)	Lini (mm)	Tension (atm)	$\theta$ ( $\text{cm}^3/\text{cm}^3$ )	Ls (cbar)	*MAD (%) **	L20 (mm)	LR (mm)
Garlic	400	87.73	0.3/0.6	0.44/0.37	13/18	34.65	14.44	28.88
Chili	600	131.60	0.3/0.6	0.44/0.37	13/18	34.65	14.44	43.32
Maize	800	128.69	0.5/0.8	0.39/0.35	17/21	46.00	8.00	32.00
Oats	600	110.76	0.4/1.0	0.41/0.33	15/24	53.57	15.69	47.06
Alfalfa	800	147.68	0.4/0.7	0.41/0.36	15/20	40.97	10.43	41.71
Bean	600	110.76	0.4/0.8	0.41/0.35	15/20	45.96	12.51	37.53

Notes: Pr=rooting or irrigation depth, Lini=establishment or initial irrigation depth, Tension=optimal soil water tension range for the crop,  $\theta$ =volumetric water content, Ls=reading from the WATERMARK 200SS moisture sensor, MAD=maximum allowable depletion for the crop, L20=irrigation depth at 20 cm soil depth, LR=required irrigation depth to reduce sensor reading from maximum to minimum threshold.

**Table 7.** Irrigation programming parameters with WATERMARK 200SS sensors for six crops from sample 2, with  $\theta_{CC}=0.12$ ,  $\theta_{PMP}=0.05$  and  $Da=1.56 \text{ g cm}^{-3}$ .

Crop	Pr (mm)	Lini (mm)	Tension (atm)	$\theta$ ( $\text{cm}^3/\text{cm}^3$ )	Ls (cbar)	*MAD (%) **	L20 (mm)	LR (mm)
Garlic	400	28.21	0.3/0.6	0.12/0.10	24/29	30.71	3.80	7.60
Chili	600	42.31	0.3/0.6	0.12/0.10	24/29	30.71	3.80	11.41
Maize	800	33.17	0.5/0.8	0.10/0.09	28/32	40.27	2.22	6.65
Oats	600	36.95	0.4/1.0	0.11/0.09	26/31	47.00	4.34	13.01
Alfalfa	800	49.26	0.4/0.7	0.11/0.09	26/31	35.96	2.82	11.29
Bean	600	36.95	0.4/0.8	0.11/0.09	26/31	40.27	3.41	10.24

**Table 8.** Irrigation programming parameters with WATERMARK 200SS sensors for six crops from sample 3, with  $\theta_{CC}=0.35$ ,  $\theta_{PMP}=0.14$  and  $Da=1.24 \text{ g cm}^{-3}$ .

Crop	Pr (mm)	Lini (mm)	Tension (atm)	$\theta$ ( $\text{cm}^3/\text{cm}^3$ )	Ls (cbar)	*MAD (%) **	L20 (mm)	LR (mm)
Garlic	400	86.53	0.3/0.6	0.35/0.30	12/16	25.65	11.19	22.39
Chili	600	129.79	0.3/0.6	0.35/0.30	12/16	25.65	11.19	33.58
Maize	800	137.55	0.5/0.8	0.31/0.28	15/18	35.84	6.86	27.44
Oats	600	114.38	0.4/1.0	0.33/0.26	14/20	43.25	13.39	40.17
Alfalfa	800	152.51	0.4/0.7	0.33/0.29	14/18	31.20	8.55	34.19
Bean	600	114.38	0.4/0.8	0.33/0.28	14/18	35.84	10.41	31.24

**Table 9.** Irrigation programming parameters with WATERMARK 200SS sensors for six crops from sample 4, with  $\theta_{CC}=0.29$ ,  $\theta_{PMP}=0.13$  and  $Da=1.23 \text{ g cm}^{-3}$ .

Crop	Pr (mm)	Lini (mm)	Tension (atm)	$\theta$ ( $\text{cm}^3/\text{cm}^3$ )	Ls (cbar)	*MAD (%) **	L20 (mm)	LR (mm)
Garlic	400	68.47	0.3/0.6	0.29/0.25	6/12	29.95	9.48	18.96
Chili	600	102.70	0.3/0.6	0.29/0.25	6/12	29.95	9.48	28.44
Maize	800	106.61	0.5/0.8	0.26/0.23	6/12	40.04	5.60	22.40
Oats	600	89.41	0.4/1.0	0.27/0.22	8/14	47.20	10.95	32.84
Alfalfa	800	119.21	0.4/0.7	0.27/0.24	8/12	35.48	7.09	28.37
Bean	600	89.41	0.4/0.8	0.27/0.23	8/12	40.04	8.59	25.78

**Table 10.** Irrigation programming parameters with WATERMARK 200SS sensors for six crops from sample 5, with  $\theta_{CC}=0.47$ ,  $\theta_{PMP}=0.27$  and  $Da=1.0 \text{ g cm}^{-3}$ .

Crop	Pr (mm)	Lini (mm)	Tension (atm)	$\theta$ ( $\text{cm}^3/\text{cm}^3$ )	Ls (cbar)	*MAD (%) **	L20 (mm)	LR (mm)
Garlic	400	86.08	0.3/0.6	0.47/0.41	10/15	31.06	12.66	25.33
Chili	600	129.11	0.3/0.6	0.47/0.41	10/15	31.06	12.66	37.99
Maize	800	131.41	0.5/0.8	0.42/0.39	14/17	41.50	7.26	29.03
Oats	600	111.12	0.4/1.0	0.44/0.37	13/19	48.75	14.21	42.62
Alfalfa	800	148.16	0.4/0.7	0.44/0.4	13/16	36.81	9.32	37.27
Bean	600	111.12	0.4/0.8	0.44/0.39	13/16	41.50	11.24	33.71

(Pr=800 mm), require higher irrigation depths (LR between 22.40 and 47.06 mm), while crops such as garlic, chili, and beans (Pr=400-600 mm) have lower water requirements. However, since they are more sensitive (low tension thresholds), they must be monitored more precisely to maintain tensions between 0.3-0.6 atm, whereas alfalfa and maize can be managed with broader ranges.

### Implementation of calibrated sensors for irrigation scheduling

The results of this study demonstrate that in situ calibration of the WATERMARK 200SS sensor is a critical step in transforming it from a generic measuring device into a robust tool for precision irrigation scheduling. The high accuracy ( $R^2 > 0.96$ ) of the calibration models developed for each soil type confirms the feasibility of overcoming the main limitation of these sensors: the influence of soil texture and structure on their readings, a challenge widely reported in the literature (Vita Serman *et al.*, 2006). By establishing soil-specific calibration curves, this work provides the necessary transfer functions to convert readings in centibars directly into volumetric moisture content the key variable for calculating irrigation depths. The effectiveness of this methodology is reflected in the broad range of calculated irrigation depths (from 7.6 mm in sandy loam to 47.06 mm in clay), highlighting the importance of tailoring irrigation not only to the crop but also to the soil's hydrophysical properties. This approach aligns with the recommendations of Yadav *et al.* (2020), who concluded that the use of soil moisture sensors can improve water use efficiency and help farmers optimize their irrigation schedules. Moreover, they

recommend sensor burial at various depths depending on the cropping season to maximize water efficiency and improve yields. Therefore, the methodology presented here offers an accessible and technically sound framework for farmers in Zacatecas to move beyond empirical irrigation practices and adopt data-driven management, thereby enhancing the resilience of production systems to water scarcity.

## CONCLUSIONS

WATERMARK 200SS<sup>®</sup> sensors are a reliable tool for irrigation scheduling in the agricultural soils of Zacatecas, adapting well to the diverse edaphic properties and water demands of the evaluated crops. Bulk density, texture, and organic matter content significantly influenced the water retention capacity of the different soil types. Sensor calibration showed excellent performance ( $R^2 > 0.96$ ), validating their accuracy in estimating moisture across varying textures. These findings highlight the potential of the WATERMARK sensor as an irrigation scheduling instrument, provided it is installed at the optimal rooting depth. However, it is recommended that field validation of the models be conducted and schedules be adjusted according to local climatic conditions and agronomic practices. Collectively, this study provides a technical foundation for implementing precision irrigation strategies aimed at improving water use efficiency and agricultural sustainability in Zacatecas.

## ACKNOWLEDGMENTS

The authors thank Aguas Firmes, implemented by the German Development Cooperation (GIZ) and promoted on behalf of the Federal Ministry for Economic Cooperation and Development of Germany (BMZ); the leading brewery AB InBev, through Grupo Modelo and Coca-Cola Company; and INIFAP. Reference numbers: SIGI 1234837220 and 135051364.

## REFERENCES

- [1] Kılıç, Z. (2020). The importance of water and conscious use of water. *International Journal of Hydrology*, 4(5), 239-241. <https://doi.org/10.15406/ijh.2020.04.00250>
- [2] Guzmán-López, F., Guerrero-Medina, M. del R., & Durán-Sosa, R. Y. (2024). Escasez hídrica en la agricultura como impacto del cambio climático en Zacatecas, México, 2000-2022. *Revista Latinoamericana de Recursos Naturales*, 20(2), 56-66.
- [3] Torres-Moreno, M., Mora-Flores, J. S., García-Salazar, J. A., Rubiños-Panta, E., Arana-Coronado, O. A., & Arjona-Suarez, E. (2023). Factores determinantes de la adopción de riego tecnificado en La Laguna, México. *Tecnología y ciencias del agua*, 14(6), 122-157. <https://doi.org/10.24850/j-tyca-14-06-04>
- [4] Servín, P. M., Tijerina, C. L., Medina, G. G., Palacios, V. O., & Flores, M. H. (2017). Sistema para programar y calendarizar el riego de los cultivos en tiempo real. *Revista mexicana de ciencias agrícolas*, 8(2), 423-430. <https://doi.org/10.29312/remexca.v8i2.61>
- [5] Bórquez-López, R.A., Valdez-Torres, L.C., Yépez-González, E., & Garatuzza-Payán, J. (2013). Calibración del sensor de matriz granular (SMG) para determinar la retención de agua en el suelo para la programación de riego en tomate en el Valle del Yaqui. *Revista Latinoamericana de Recursos Naturales*, 9(1), 11-16.
- [6] Abdelfattah, A. H., Sabirov, R. F., Ivanov, B. L., Lushnov, M. A., & Sabirov, R. A. (2020). Calibration of soil humidity sensors of automatic irrigation controller. In *BIO Web of Conferences* (Vol. 17, p. 00249). <https://doi.org/10.1051/bioconf/20201700249>
- [7] Chavarría-Vidal, A. E., Morales-Sánchez, M., & Soto-Bravo, F. (2024). Efecto de diferentes tensiones del agua en el suelo sobre la absorción nutricional de macronutrientes en el cultivo de cebolla (*Allium cepa*) cv Álvara en ambiente protegido. *Revista Tecnología en Marcha*, 37(1), 3-16. <https://dx.doi.org/10.18845/tm.v37i1.6428>

- [8] Bedard-Haughn, A. (2009). Managing excess water in Canadian prairie soils: A review. *Canadian Journal of Soil Science*, 89(2): 157-168. <https://doi.org/10.4141/CJSS07071>
- [9] Tudor, S., Marce, D., & Hoble, A. (2013). Review for Soil with Excess Moisture. *ProEnvironment* 6(2013) 495-498.
- [10] Galdeano L., L. J., Robles R., C. O., Vargas C., D., & Servin P., M. (2024). Calibración del sensor Watermark 200SS y Tensiómetro para programación de riego, Caso de estudio: Textura arenosa. En IX CONGRESO NACIONAL Y II CONGRESO INTERNACIONAL DE RIEGO, DRENAJE Y BIOSISTEMAS (COMI), México.
- [11] Medina, A., García, M. A., Varela, S. E., Ramírez, J. A., & Ruvalcaba, L. G. (2018). Calibración de sensores de resistencia en la medición del potencial mátrico en tres tipos de suelos en condiciones de invernadero. *AgroProductividad*, 11(9), 137-143. DOI: <https://doi.org/10.32854/agrop.v11i9.1226>
- [12] Tartaglia, M., Pirone, M., & Urciuoli, G. (2023). Calibration of a granular matrix sensor for suction measurements in partially saturated pyroclastic soil. *E3S Web of Conferences* 382, 22004. <https://doi.org/10.1051/e3sconf/202338222004>
- [13] Irrrometer. (2024). Medidor digital Irrrometer. <https://www.irrometer.com/pdf/407sp.pdf>
- [14] Soham A., Neeraj R., K Sri H., Shivam T., Markus D., & Saket P. (2019). Laboratory calibration of soil moisture sensors in porous media (repacked soils). *Protocols.io*. <https://dx.doi.org/10.17504/protocols.io.swnefde>
- [15] Starr, J.L., & Paltineanu, I.C. (2002). Methods for measurement of soil water content: capacitance devices. In *Methods of soil analysis. Part 4. Physical methods*. Edited by J.H. Dane and G.C. Topp. Soil Science Society of America. pp. 463-474.
- [16] Catalán V., E.A.; Sánchez C., I.; Villa C., M.M.; Inzunza I., M.A. y Mendoza M., S.F. 2007. Programa para calcular demandas de agua calendarizar el riego de los cultivos. Folleto técnico 7. INIFAP CENID RASPA. Gómez Palacio, Durango.
- [17] Servín P., M., Tijerina C., L., Medina G., G., Palacios V., O., & Flores M., H. (2017). System to program and schedule the irrigation of crops in real time. *Revista mexicana de ciencias agrícolas*, 8(2), 423-430.
- [18] United States Department of Agriculture (USDA). 1999. Bulk Density, in: *Soil Quality Test Kit Guide*. Agricultural Research Service. Natural Resources Conservation Service. Soil Quality Institute. Auburn, AL, USA. pp. 9-13. [https://efotg.sc.egov.usda.gov/references/public/WI/Soil\\_Quality\\_Test\\_Kit\\_Guide.pdf](https://efotg.sc.egov.usda.gov/references/public/WI/Soil_Quality_Test_Kit_Guide.pdf)
- [19] Hartati, W., & Sudarmadji, T. (2016). Relationship between soil texture and soil organic matter content on mined-out lands in Berau, East Kalimantan, Indonesia. *Nusantara Bioscience*, 8(1), 83-88. <https://doi.org/10.13057/NUSBIOSCI/N080115>.
- [20] Vita Serman, F., Schugurensky, C., Carrión, R., & Rodríguez, S. (2006). Evaluación del comportamiento de sensores de humedad de suelo del tipo (FDR) de desarrollo local, en relación al contenido de agua ya la textura de suelo. *JORNADAS DE ACTUALIZACIÓN EN RIEGO Y FERTIRRIEGO*, 3.
- [21] Yadav, P. K., Sharma, F. C., Thao, T., & Goorahoo, D. (2020). Soil moisture sensor-based irrigation scheduling to optimize water use efficiency in vegetables. *Irrig. Assoc*, 1-7.